A MODEL OF A DIPOLE ANTENNA IN A 3-D FDTD SPACE

Ioana SĂRĂCUȚ Victor POPESCU
Technical University of Cluj-Napoca,
G. Bariţiu Street 26-28, Cluj-Napoca, phone 0264-401803
e-mail: Ioana.Saracut@bel.utcluj.ro

Abstract: In this paper a dipole antenna with a gap is modeled in a 3-D Finite–Difference Time-Domain coordinate space surrounded by Perfectly Matched Layer (PML). Unlike the analytical study, where the sinusoidal distribution of the current is imposed, here the propagation of direct and reflected waves of current and potential was modeled, so distribution along the antenna resulted from simulations. The simulation results include the radiation pattern, the transitory state of the field and the effect of the conductor losses.

Keywords: *dipole antenna, Finite-Difference Time-Domain, Perfectly Matched Layer, Matlab model.*

I. INTRODUCTION

Dipole antenna has been studied in detail, given the particular function of distance transmission. As a result, attention was focused on the phenomena in the far field region and less on what is happening in the vicinity of the antenna field. Given the purpose, the technique used was based on a series of approximations. For example, in [1], a sinusoidal current distribution through an ideal antenna is considered; both the conductor diameter and the gap between the two elements are neglected.

The purpose of this paper is to model a dipole antenna with a feeding gap and to simulate it in an infinite, homogeneous, isotropic 3-D medium, without imposing a sinusoidal current distribution. The antenna is modeled using the analogy with the long lines equations and connects to the field model, which is realized using the electromagnetic field theory.

For the modeling of the space in Matlab, we used the *Finite-Difference Time-Domain* (FDTD) method, a volume discretization technique introduced by Kane S. Yee in 1966 [2]. A 3-D FDTD simulated space is divided into identical cubic cells of side Δx, called *Yee cells*. In a Yee cell, the electric field components are positioned in the middle of the edges of the cube, and the magnetic field components are positioned in the center of the faces.

In order to simulate the propagation of the electromagnetic energy in an infinite space, the space was truncate by using the *Perfectly Matched Layer* (PML) technique, proposed by J.P. Berenger in 1994 [3]. The PML is a nonphysical absorber layer which is placed adjacent to the edges of the FDTD grid and attenuates by absorption all the waves that enter into this layer. The accuracy of the PML technique was verified in 2-D FDTD coordinate space [3] and in 3-D grids [4]-[9].

The present paper continues the partial study of the dipole antenna initiated in [10], with a more rigorous model of the phenomena that occur inside and near the dipole antenna.

Section II of this paper presents the calculation of the correct input resistance for a dipole antenna with gap. Section III explains the Matlab modeling of the antenna and the parameters that control its connection to the FDTD space. In Section IV the simulation results are presented, including the radiation pattern, the transitory state of the field and the effect of the conductor losses. Finally, Section V gives some concluding remarks.

II. THE CORRECTION OF THE INPUT RESISTANCE

Consider a dipole antenna of length L, in an infinite, isotropic and homogeneous space. Considering a sinusoidal current distribution through the antenna, the ideal input resistance R_{id} can be written as [1]:

$$R_{id} = \frac{R_{rad}}{sin^2\left(k_L \pi\right)} \tag{1}$$

where R_{rad} is the radiation resistance and k_L is the length factor of the antenna:

$$k_L = \frac{L}{\lambda} \tag{2}$$

where λ is the wavelength.

The above refers to the ideal dipole antenna, in particular *no gap* between its two elements. Certainly,

This work was supported by the Romanian University Research Council CNCSIS, within the PNII–IDEI framework, grant no. 2534/ 2008.

Manuscript received October 25, 2011; revised November 28, 2011

such an antenna cannot be obtained either in practice or in modeling (two potentially should be defined in the same point – the middle point). In practice, the nominal length of the dipole antenna includes the gap; therefore the length factor refers to the total length. The model presented in this paper has a gap of length *a*, which is a fraction of the dipole length (see *Figure 1*, where half of the gap is represented, i.e. $a/2$) .

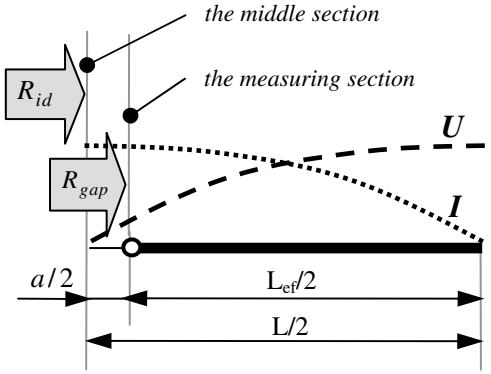

Figure 1. The correct measuring of the input reactance for a dipole with gap

The input resistance is not measured in the center of the antenna (the *middle section* in the figure), but $a/2$ away from it (*the measuring section*). As a result, the input resistance of the antenna with gap (R_{gap}) is greater than the input resistance of the antenna without gap (R_{id}). To use the theoretical graphs in model's calibration, the input resistance must be calculated for an "effective" length factor which is higher than if the gap is neglected:

$$k_{Lc} = \frac{L}{L_{ef}} \cdot k_L = \frac{L}{L-a} \cdot k_L \qquad (3)$$

where L_{ef} is the effective length of the dipole antenna. *Figure 2* illustrates the input resistance R_{id} of the ideal dipole antenna, i.e. without gap (dashed line), and the input resistance R_{gap} of a dipole antenna with a gap of *10%* (continuous line) both versus the length factor. As an example, for $k_L = 0.5$ the input resistance increases from *73* Ω for the ideal dipole antenna to *98* Ω for the model analyzed here.

III. MODELING OF DIPOLE ANTENNA

Consider a dipole antenna in a 3-D FDTD space bounded by a PML modeling an infinite, isotropic and homogeneous medium. The antenna is placed in the plane (*yOz*), parallel to *z*-axis, one cell away from the PML and positioned symmetrically about the plane (*xOy*), as seen in *Figure 3.*

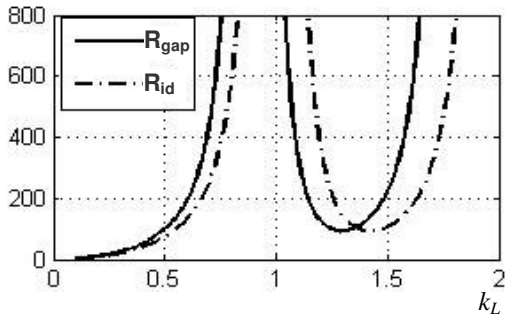

Figure 2. The input resistance of the dipole antenna without gap (R_{id}) *and the input resistance of a dipole with a gap of 10 %* (R_{gap}) *versus the length factor .*

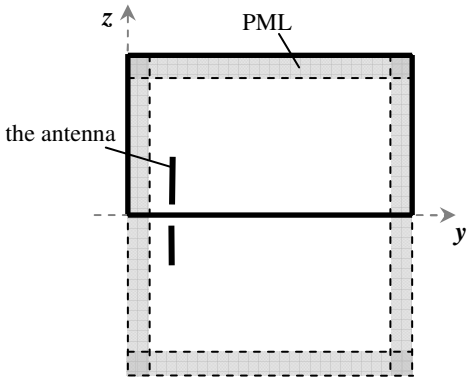

Figure 3. The dipole antenna in the infinite 3-D space (the outlined rectangle represents the modeled space).

The absorption in PML is considered as a polynomial function of the depth (*y*) in PML [10]:

$$a(y) = 1 - \frac{1-a_{min}}{g^2} \cdot y^2 \qquad (4)$$

where *g* is the thickness of the PML and a_{min} is the minimum attenuation in PML ($0 < a_{min} < 1$).

If the antenna emits in a homogeneous and isotropic space, the resulted field is symmetric to the plane (*xOy*). Moreover, the plane of symmetry is an equipotential plane, so the image method can be used: only half the space was modeled considering the area (*xOy*) as conductor (the outlined rectangle in *Figure 3*). In this case, the field distribution between the conductor plane and dipole element is the same as between the two elements in the absence of the conductor plane.

The simulated space was divided into cubic Yee cells and the dipole antenna was divided into segments. The dipole antenna was placed so that a segment is on an edge of a Yee cell, oriented along the *z*-axis, and it connects to the electromagnetic field through the nearby field components (*Figure 4*). We mention that in *Figure 4* only some of the field components have been presented in

order to simplify the depiction. The electric current of dipole segments determines the magnetic field in proximity (H_x, H_y) and also the movement of electrical charges. Since the currents in two adjacent segments are not generally equal, accumulation of electric charge (q) will occur at the end segments. These charges will result in an electric field (E_x, E_y).

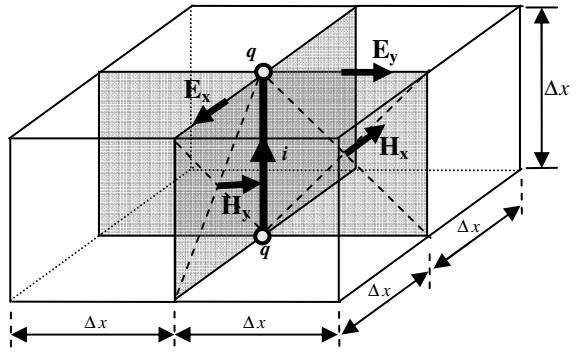

Figure 4. The connection of one segment of the dipole to the FDTD space.

The antenna modeling must also solve the problem of the *interface* between the antenna and the electromagnetic field. The time step was chosen so that the wave travels the distance equal to Δx in two time increments [10]. Therefore, to match the speed of wave propagation along the antenna with the propagation in space, the phenomena along the antenna must be analyzed at twice higher the resolution. The conversion from one resolution to the other was done by over-/under-sampling, using the cubic interpolation to increase the precision. Interpolation was necessary because the field components are defined at different points for each resolution, as seen in *Figure 5* for H.

The radiated power was evaluated in two steps: first the power density was calculated on a closed surface (a sphere) surrounding the antenna; then the power density was integrated on the surface considered. Instantaneous power density is determined by the field components, but there were two inconveniences:

- The network is discrete; therefore the points where the field is calculated directly are located alternately on one side and on the other of an ideal arc of a circle.
- The pair (E, H) is calculated at different points, so direct calculation of power density (using the Poynting vector) leads to errors.

Both problems were simultaneously solved using the linear interpolation and the cubic interpolation. If the antenna radiates in a homogeneous and isotropic medium, the field has a rotational symmetry: the field is the same in any plane along the antenna's axis. In this case, the field can be studied in only one of these planes and we chose the plane (yOz). The intersection of the spherical surface with this plane is a curve (*Figure 6*); the surface itself can be obtained by rotating this curve around the z-axis.

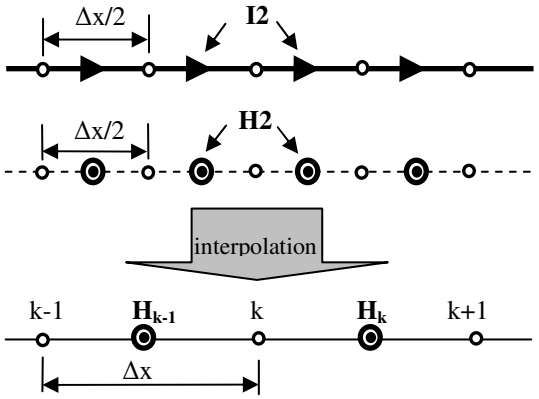

Figure 5. The currents through the dipole (I2), the magnetic field at double resolution (H2) and the magnetic field at Yee's resolution (H).

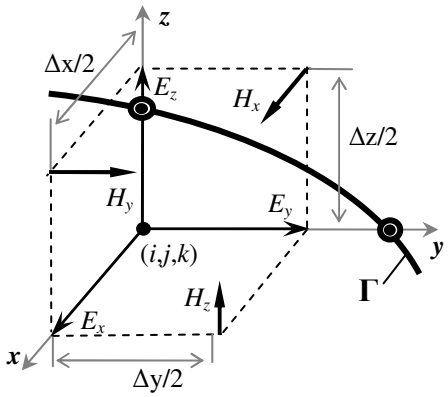

Figure 6. The radiated power was calculated on the curve Γ by using the interpolation.

Considering a sinusoidal signal applied as excitation, current distribution in an element is following the same current distribution as in an open-circuited transmission line (the current at the end of the element tends to zero). Feeding the antenna at the center, it generates waves that propagate to its ends, where reflections occur; reflected wave meets with the direct wave, forming standing waves. They have two minima at each antenna end – for the current wave – and two maxima – for the voltage wave respectively.

The study of the field radiated by an antenna is usually based on simplifying the phenomena that occur in the antenna. For example, in [1] the antenna current distribution is given and the magnetic vector potential is determined in different points in space; the magnetic field results and then the electric field is derived from Maxwell's equations. This does not take into account the complexity of the phenomena that occur in the antenna

because the aim is not to model it, but to study the field around it.

The purpose was to develop a model for the antenna using the circuit theory and then to connect it to the field model, realized with the electromagnetic field theory. For this purpose, two pairs of parameters were introduced:

- k_{IV} and k_{VI} control the relationship between currents and potentials of the antenna;
- k_{EV} and k_{HI} control the connection of the antenna to the electromagnetic field.

Through some preliminary tests, we determined the values of these parameters so that both the stability of the model and the input resistance are ensured.

A. Choosing of parameters k_{IV} and k_{VI}

First a dipole segment of the antenna was equated with an electrical circuit (*Figure 7*).

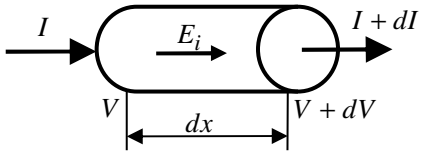

Figure 7. The equivalent circuit of a dipole's segment

By applying Ohm's law it follows that:

$$\begin{cases} \dfrac{dI}{dt} + \dfrac{1}{\tau}\cdot I = -\dfrac{1}{L}\left(dV - E_i dz\right) \\ \dfrac{dV}{dt} = -K\cdot dI \end{cases} \tag{5}$$

where V is the potential due to the local accumulation of electric charges, $\tau = \dfrac{L}{R}$ is a time constant, E_i is the induced electric field and K is a proportionality constant. By discretization the iterative relations result:

$$\begin{cases} I_k^{(n+1)} = \alpha_P \cdot I_k^{(n)} + k_{IV}\left(V_k^{(n)} - V_{k-1}^{(n)} + E_{i,k}^{(n)}\cdot\Delta x\right) \\ V_k^{(n+1)} = V_k^{(n)} + k_{VI}\left(I_k^{(n)} - I_{k-1}^{(n)}\right) \end{cases} \tag{6}$$

where:

- the current $I_k^{(n)}$ and the potential $V_k^{(n)}$ are measured in node k of the antenna segment, at the moment n of sampling;
- $k_{IV} = \dfrac{\Delta t}{L}$ and $k_{VI} = K\Delta t$;
- $\alpha_P = 1 - \dfrac{\Delta t}{\tau}$ is a factor that controls the losses on the resistance of the conductor, as it will be shown in Section IV of this paper.

Considering Maxwell's equations for a plane electromagnetic wave having only the components H_x and E_z, the discretized equations result:

$$\begin{cases} H_k^{n+1} = H_k^n + \dfrac{\Delta t}{\mu\cdot\Delta x}\left(E_k^n - E_{k-1}^n\right) \\ E_k^{n+1} = E_k^n + \dfrac{\Delta t}{\varepsilon\cdot\Delta x}\left(H_k^n - H_{k-1}^n\right) \end{cases} \tag{7}$$

By comparing (6) and (7), the following correspondences by analogy result:

$$\begin{cases} k_{IV} \leftrightarrow \dfrac{\Delta t}{\mu\cdot\Delta x} \\ k_{VI} \leftrightarrow \dfrac{\Delta t}{\varepsilon\cdot\Delta x} \end{cases} \tag{8}$$

It follows that:

$$\begin{cases} k_{IV}k_{VI} \leftrightarrow \dfrac{1}{\mu\cdot\varepsilon\cdot v^2} \\ \dfrac{k_{VI}}{k_{IV}} \leftrightarrow Z_0^2 \end{cases} \tag{9}$$

where $v = \dfrac{\Delta x}{\Delta t} = \dfrac{1}{\sqrt{\mu\varepsilon}}$ is the speed of propagation of waves along the antenna and $Z_0 = \dfrac{\mu}{\varepsilon}$ is the wave impedance, in particular the input reactance. Using (9) two new parameters were introduced:

$$\begin{cases} k_{VI}\cdot k_{IV} = sp^2 \\ \dfrac{k_{VI}}{k_{IV}} = R_0^2 \end{cases} \tag{10}$$

In the following we will explain how these two parameters (sp and R_0) were chosen.

Due to the fact that the standing waves are synchronous, a propagation phenomenon of the resulting wave should not occur. Propagation occurs for $sp < 1$ and the phenomenon is more pronounced as sp decreases. If $sp = 1$, the model becomes unstable. The results show that there is a good compromise for $sp = 0.998$.

The parameter R_0 was found in a few steps: first, the model has been run with an arbitrary value R_0'; taking into account the input resistance R_{in}^m and the theoretical input resistance (1), R_0 is given by:

$$R_0 = \frac{R_{id}}{R_{in}^m}\cdot R_0' \tag{11}$$

It should be noticed that the above proportionality is kept as long as remain parameters have no longer suffer from any changes. If proportionality would be maintained regardless of the others parameters' values, this would overload the task of R_0 finding.

The gap size is fixed (one cell) and its weight in the dipole's length is adjusted by choosing the number of segments (cells) on the dipole element. Thus *nseg* cells on one element (without gap) results in a gap of :

$$d = \frac{1}{n+1} \cdot 100 \ [\%] \tag{12}$$

Table 1 shows the results obtained in Matlab for the radiance resistance (R_{rad}), the input resistance (R_{gap}) and R_0, for a few values of the gap (*d*) and the length factor.

Table 1. Results obtained in Matlab

nseg	*5*	*7*	*9*	*11*	*13*	*15*
$d\ [\%]$	16.67	12.5	10.00	8.33	7.14	6.25
$k_L = 0.5$						
$R_{rad}\ [\Omega]$	137	121	113	107	104	101
$R_{gap}\ [\Omega]$	151	128	116	110	105	102
R_0	836	548	441	389	357	337
$k_L = 0.6$						
$R_{rad}\ [\Omega]$	196	181	171	165	161	158
$R_{gap}\ [\Omega]$	330	259	228	211	200	193
R_0	1000	743	638	585	549	522
$k_L = 0.7$						
$R_{rad}\ [\Omega]$	229	222	216	212	209	206
$R_{gap}\ [\Omega]$	986	642	523	464	428	403
R_0	2145	1235	909	758	682	625
$k_L = 0.8$						
$R_{rad}\ [\Omega]$	222	229	231	231	231	230
$R_{gap}\ [\Omega]$	14137	3243	1976	1526	1299	1164
R_0	4781	3806	2267	1712	1440	1274

After establishing the values of *sp* and R_0, k_{IV} and k_{VI} result from (10).

B. Choosing of parameters k_{EV} and k_{HI}

These two parameters weights the link between the currents and the potentials of the antenna and the field quantities, controlling in fact the power transfer between the two elements of the model.

$$\begin{aligned} E_k &= k_{EV} \cdot V_k \\ H_k &= k_{HI} \cdot I_k \end{aligned} \tag{13}$$

To calibrate the relationship between the antenna and the electromagnetic field, the parameters k_{EV} and k_{HI} were determined in the following conditions: the length factor of the antenna $k_L = 0.5$, the number of segments on an element $nseg = 10$, the size of the modeled space: $X \times Y \times Z = 1\lambda \times 3\lambda \times 2\lambda$, the radius of the sphere for the calculus of powers $r = 2\lambda$, PML's thickness $g = 10$ cells and the minimum attenuation in PML $a_{\min} = 0.4$. The parameter R_0 has been chosen so that the input resistance is about 98 Ω (see *Figure 1*). We mention here that *nseg* represents the number of segments on an element plus one cell representing the gap, thus the resolution results of *40* cells / wavelength.

At the input of the antenna, the following quantities were measured: the input impedance $Z_{in} = 134\ \Omega$, the input phase shift $\varphi_{in} = -43°$, the measured input resistance $R_{in}^m = 97.5\ \Omega$ and the input power $P_{in} = 10.84\ mW$. All these parameters remained constant during the simulations.

The Matlab program allows excitation field either by the electric component or by the magnetic component or both. Five tests were run until the total power radiated P_{rad} and the total error power ε_p from the power measured at input:

- *Test 1*: The field was excited only by the magnetic component ($k_{HI} \neq 0$ and $k_{EV} = 0$). Starting with an arbitrary value k_{HI0}, the radiated and the input powers were measured (P_{rad} and P_{in}) ; the parameter k_{HI} was calculated as:

$$k_{HI} = k_{HI0} \sqrt{\frac{P_{in}}{P_{rad}}} \tag{14}$$

- *Test 2*: Similarly as test 1, but for the electric component.
- *Test 3*: The field was excited by both component, electric and magnetic, but maintaining previously defined values of k_{EV} and k_{HI} ; the error resulted very high.
- *Test 4*: The parameter values have been cut to a half and the power radiated error resulted still high. In conclusion, the two parameters must be determined again.
- *Test 5*: In the last test this calibration was performed.

The results of the tests are presented in *Table 2.*

Given that k_{EV} and k_{HI} have remarkably close values, tests were done where the two parameters are equal. The results are shown in *Table 3* for a few values of the gap. It should be noticed that the power measured in the field differs by less than 1% of the input power. Also, the input resistance is very close to the case when $k_{EV} \neq k_{HI}$.

Table 2. The resulted values of k_{EV} and k_{HI}

test	1	2	3	4	5
k_{HI}	12.872	0	12.872	6.436	6.710
k_{EV}	0	13.775	13.775	6.887	7.188
P_{rad} [mW]	10.985	10.877	42.453	9.88	10.809
ε_p [%]	+1.34	+0.34	+392	-8.85	-0.29

Table 3. The results when $k_{EV} = k_{HI}$

nseg	5	7	9	11	13	15
d[%]	16.67	12.5	10.00	8.33	7.14	6.25
k_{HI} k_{EV}	4.5243	5.6835	6.5652	7.3195	8.0022	8.5819
P_{in}	1.6793	4.9548	8.2455	10.976	13.134	14.761
P_{out}	1.6715	4.9515	8.1879	10.877	13.112	14.769
ε_P[%]	-0.46	-0.07	-0.70	-0.90	-0.17	+0.05
φ[°]	-69	-55.69	-46.35	-39.37	-34.07	-30.09
R_{in}	152.95	128.26	115.57	108.88	104.48	101.43
ε_r[%]	+1.29	+0.20	-0.37	-1.02	-0.49	-0.69

IV. THE SIMULATIONS RESULTS

A. The radiation pattern

The radiation pattern was calculated using the interpolation for the electric and magnetic components computing on the sphere as mentioned above. The duration of the simulation was chosen so that it is longer than the transitory state at the sphere:

$$T_{sim} > T_{prop} + T_{tranz} + T_{per} \tag{15}$$

where:

- T_{sim} is the total duration of the simulation;
- T_{prop} is the necessary time for the wave to propagate from the antenna to the sphere;
- T_{trans} is the duration of the transitory state at the sphere;
- T_{per} is the period of the excitation.

Figure 8.a shows the polar radiation pattern analytically determined (continuous line) and the one measured on the model (dashed line). It should be noticed that the overlap is quite good. For quantitative assessments of errors the power density versus the angle to the antenna's axis was represented in Cartesian coordinates (*Figure 8.b*). The mean square error is *0.024%*.

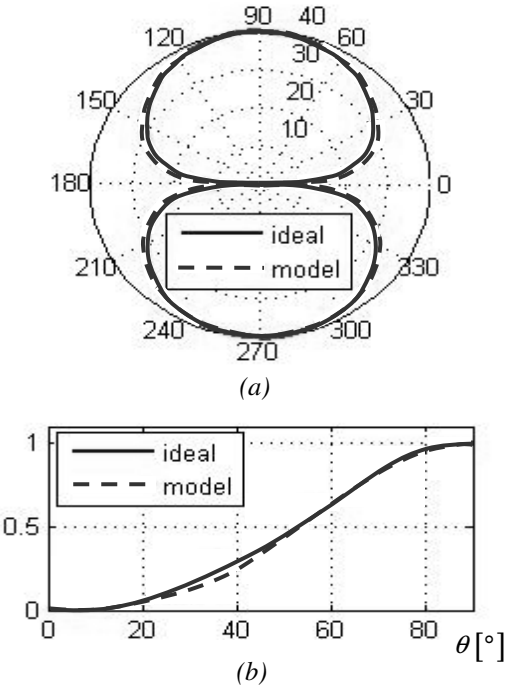

Figure 8. The radiation pattern: (a) polar representation (in dB); (b) linear representation.

B. The current and the potential along the antenna

The envelopes of the local oscillations are represented by the current and the potential distribution along the antenna. For an ideal antenna, both are sinusoidal. In the analytical study, the sinusoidal distribution is imposed; here, the propagation of direct and reflected waves of current and potential was modeled, so their distributions along the antenna resulted from simulations as shown in *Figure 9*.

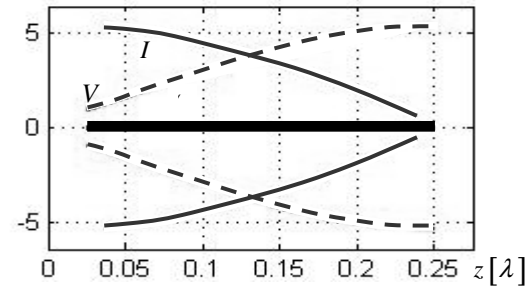

Figure 9. Current and potential distribution along the dipole.

The variable z on the abscissa represents the distance from the middle of the antenna, measured in fractions of wavelength (electric distance). Graph corresponds to a dipole in $\lambda/2$ (normalization length), so for a half of the element the length is $\lambda/4$ (the horizontal bold grey line in *Figure 9*). Obviously, the potentials are not numerically equal to the currents; here they were scaled to

the size of the graph. Notice the following: distribution is (approximately) sinusoidal; at the dipole extremity, the current has a minimum and the potential has a maximum; input variables depend on the length factor and the gap.

In conclusion, the results obtained with the proposed model correspond to those obtained analytically according to the mathematical model of the dipole antenna.

C. The transitory state

If the excitation is a sinusoidal signal with *a unit step envelope* then the transitory state last longer as can be seen in *Figure 10.a.*

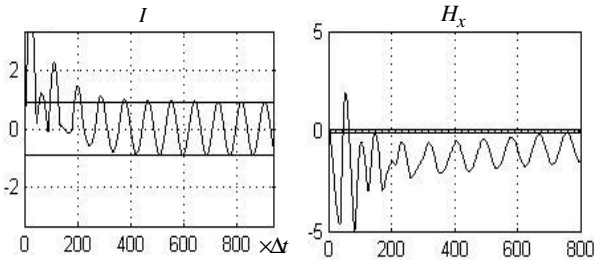

(a) unit step envelope

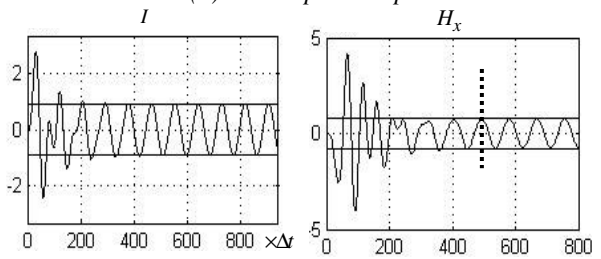

(b) raised cosine envelope for one period

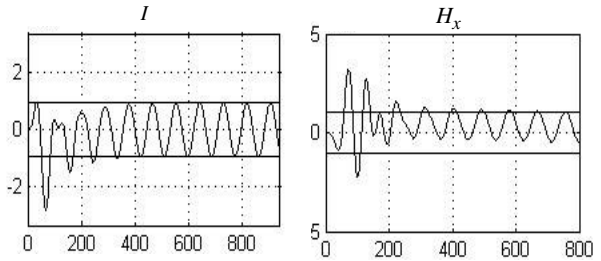

(c) raised cosine envelope for 2 periods

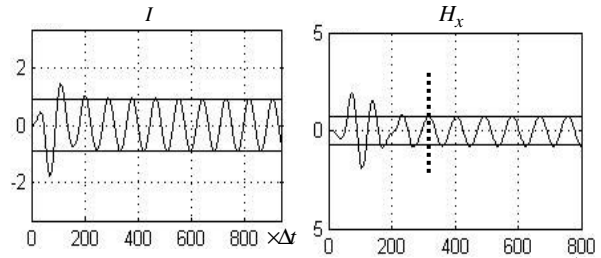

(d) raised cosine envelope for 3 periods

Figure 10. The transitory state for different types of excitations

Beside this it is interesting to notice that the transitory state of the input current is relatively short (about *5* periods of the excitation), while the transitory state of the field H_x measured at the distance of 2λ from the antenna is much longer.

Figure 10.b-d illustrate the results obtained when the excitation has *a raised cosine front*, with a duration of one, two and three periods respectively. If the duration of the front raised-cosine is equal to an even number of excitation periods, the transitory state has duration comparable to the unit step front case, so no improvement occurs. If, however, there is an odd number of time periods, the transitory state significantly shortens.

In conclusion, the optimal duration of the front is *3* periods, when the transitory state is shortening by *4* times. Obviously, the front duration cannot be increased more because it would exceed the duration of the transitory state.

D. The effects of the conductor losses

Energy losses in the conductor of the antenna are reflected in the parameter α_P, introduced in (6). *Figure 11* illustrates the voltage and the current at the input of the antenna, in the case $\alpha_P = 1$ (theoretically lossless). As expected, the voltage (with simple line) has a sinusoidal time-variation (the upper graph) and consequently one single spectral line (the lower graph) at the excitation frequency of *1 GHz* (indicated by an error of *0.51%*).

As for the current (with thick line), it looks like a double side band (DSB) modulated signal (the upper graph of *Figure 11*); this appearance of DSB signal is reflected in the frequency representation by the existence of two spectral lines at the frequencies of *1 GHz* and *1.073 GHz* respectively (the lower graph of *Figure 11*).

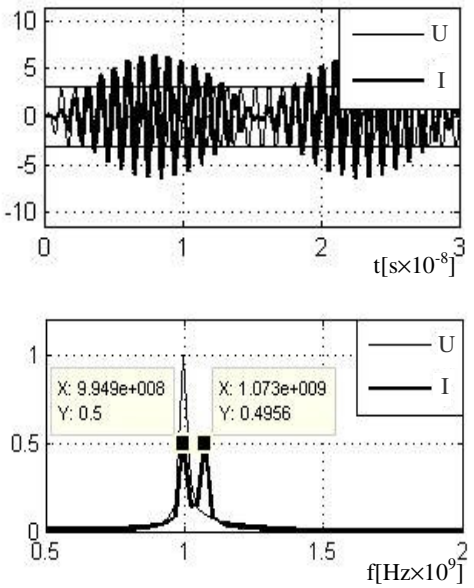

Figure 11. The voltage and the current at the input of the antenna, for $\alpha_P = 1$

To locate the cause of this disturbance, we specify that our algorithm that models phenomena in the antenna has two elements that help to ensure stability of the model:

- *the loop gain*, controlled by k_{IV} and k_{VI} (for which we chose $k_{VI} \cdot k_{IV} = 0.998$);
- *the losses in the conductor*, controlled by α_P.

From the relation $\alpha_P = 1 - \frac{\Delta t}{\tau}$ it results that the value $\alpha_P = 1$ implies $\Delta t = 0$, hence a theoretically infinite speed propagation. For this reason, we chose $\alpha_P = 0.99$ and thus the disturbance has diminished, as it can be seen both in time and frequency representations from *Figure 12*.

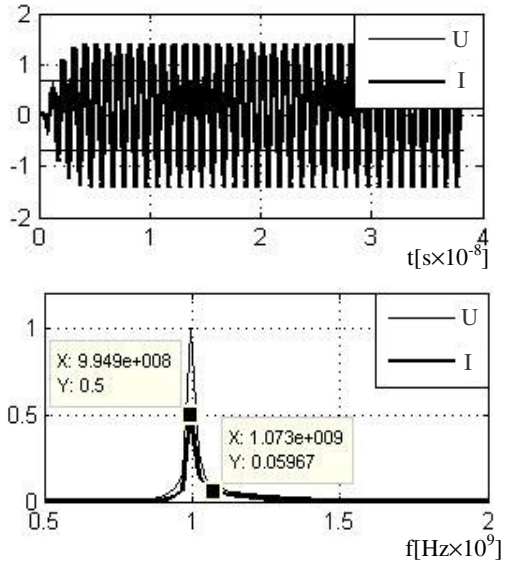

Figure 12. The voltage and the current at the input of the antenna, for $\alpha_P = 0.99$

IV. CONCLUSIONS

In this paper the radiation of a dipole antenna with a nonzero gap in an infinite, isotropic and homogeneous medium was simulated in Matlab. Unlike the analytical study, the sinusoidal current distribution was not imposed, but resulted from simulations. The model of the antenna was connected to the 3-D Finite-Difference Time-Domain coordinate space and 4 parameters were defined in order to control the modeling. The Perfectly Matching Layer technique was used in simulation of the infinite space.

The polar radiation pattern of the dipole antenna model resulted very similar to that determined analytically, achieving a mean square error of *0.024%*. The transitory state was studied for the excitation having a unit step front and a raised cosine. It was shown that the transitory state is reduced to 4 times when the duration of the excitation front is 3 periods. Another distinctive result of this work is the control of the energy losses in the conductor of the antenna by using the parameter α_P. The theoretically ideal value $\alpha_P = 1$ leads to a non-sinusoidal input current. Its appearance of DSB modulated signal has been diminished by setting α_P to *0.99*.

REFERENCES

[1] C. A. Balanis, "*Antenna Theory. Analysis and Design – 2nd ed.* ", John Wiley & Sons, Inc., New York, 1997.
[2] K. S. Yee, "*Numerical Solution of Initial Boundary Value Problems Involving Maxwell's Equations in Isotropic Media*", IEEE Transactions on Antennas and Propagation, vol. AP-14, no.8, pp.302-307, May 1966.
[3] J. P. Berenger, "*A Perfectly Matched Layer for the Absorption of Electromagnetic waves*", J.Computational Physics, vol.114, pp.185-200, Oct. 1994.
[4] D. S. Katz, T. T. Thiele, A. Taflove, "*Validation and Extension to Three Dimensions of the Berenger PML Absorbing Boundary Condition for FD-TD Meshes*", IEEE Microwave and Guided Wave Letters, vol.4, no.8, pp.268-270, Aug. 1994.
[5] J. P. Berenger, "*Evanescent Waves in PML's: Origin of the Numerical Refletion in Wave-Structure Interaction Problems*", IEEE APS, vol.47, pp.1497-1503, Oct. 1999.
[6] J. P. Berenger, "*Numerical Reflections from FDTD-PML's: A Comparison of the Split PML with the Unsplit and CFSPMLs*", IEEE APS, vol. 50, pp.258-265, March 2002.
[7] D.S. Katz, T.T. Thiele, A. Taflove, "*Validation and Extension to Three Dimensions of the Berenger PML Absorbing Boundary Condition for FD-TD Meshes*", IEEE Microwave and Guided Wave Letters, vol.4, no.8, pp.268-270, Aug. 1994.
[8] E.L. Lindman, "*Free Space Boundary Conditions of the Time Dependent Wave Equation*", J.Computational Phys., vol.18, pp.66-78, 1975.
[9] P.A. Tirkas, C.A. Balanis, "*Higher-Order Absorbing Boundary Conditions in FDTD Method*", IEEE Transactions on Antennas and Propagation, vol.40, no.10, pp.1215-1222, October 1992.
[10] I. Sărăcuț, V. Popescu, D. O. Micu, "*A Simulation of the Perfectly Matched Layer in the 3-D Case*", Acta Tehnica Napocensis – Electronics and Telecommunications, vol. 51, nr. 2, pp. 20-25, Cluj-Napoca, 2010.